Molecular Rulers

DOI: 10.1002/anie.201002943

A Quantum-Dot-Based Molecular Ruler for Multiplexed Optical Analysis**

*Frank Morgner, Daniel Geißler, Stefan Stufler, Nathaniel G. Butlin, Hans-Gerd Löhmannsröben, and Niko Hildebrandt**

In memory of Theodor Förster on the centenary of his birth on May 15th 2010

Applications based on Förster resonance energy transfer (FRET) play an important role in the determination of concentrations and distances within nanometer-scale systems in vitro and in vivo in the fields of biology, biochemistry, medicine, and other life sciences.[1–3] Due to the r^{-6} distance dependence of FRET, structural changes of molecular systems in the 1–10 nm range can be measured with high accuracy far below the light diffraction limit. Stryer et al.[4,5] demonstrated the spectroscopic ruler FRET technique more than 40 years ago, and it is still frequently used for in- and ex-vivo studies of inter- and intramolecular interactions by spectroscopy and microscopy down to the single-molecule level.[6–9] Several FRET-based biosensors for functional intracellular investigations have been developed.[10–14] Although most of these applications use single sensors, there have been some recent developments of dual FRET pairs for cellular imaging using fluorescent proteins,[15–17] and even with a single excitation wavelength.[18] Using a multiplexed FRET technique allows the simultaneous measurement of multiple distances or conformational changes, thereby decreasing time and effort whilst increasing bioanalytical information due to the possible correlation of simultaneous events.

The FRET pair combination of luminescent terbium complexes (LTCs) as donors and semiconductor quantum dots (QDs) as acceptors holds significant advantages concerning sensitivity, distance, and multiparametric analysis compared to other donor–acceptor pairs.[19,20] Due to large overlap integral values, exceptionally long Förster radii (R_0, the donor–acceptor distance at which the FRET efficiency is 50 %) of up to 11 nm can be achieved,[21–23] whereas conventional donor–acceptor pairs have much smaller R_0 values that rarely exceed 6 nm.[24] Although nanoplasmonic molecular rulers have been developed for which distances of up to about 70 nm can be measured,[25,26] these applications use relatively large noble metal nanoparticles (up to 40 nm) and are restricted in their multiplexed use of simultaneously measuring variable distances of different systems (for example, several different intracellular functional events within one measurement). The pioneering work of Weiss et al. demonstrated multiplexed optical rulers using quantum dots and ultrahigh-resolution colocalization (UHRC).[27] Although FRET has advantages concerning resolution accuracy and dynamic measurements,[28] UHRC is well-suited to measuring distances in the range of few nanometers to tens of micrometers.[29]

Two very important aspects for intracellular studies with QDs are the shape and the size of these nanosensors, which can be crucial, for example, for cell penetration and for evaluation of the nanoparticle impact on the targeted biomolecules. Measuring the core/shell dimensions of the semiconductor material with TEM is possible with relatively good accuracy. However, the equipment is rather expensive and the experiments are time-consuming and usually not performed under the same conditions as the bioanalytical studies of interest (such as live-cell imaging). Moreover, it is very difficult to acquire accurate dimensions for the entire biocompatible QD (for example including polymer coating and biofunctionalization), and TEM provides only two-dimensional images. For their polymer coated Qdots, Invitrogen provides hydrodynamic diameters (Table 1) measured by size-exclusion chromatography on HPLC, where the sizes are determined by retention time relative to a standard curve of proteins. Although this is an estimation of the overall size, the shape is not taken into account, and the values become rather inaccurate for QDs with elongated (ellipsoidal rather than spherical) shapes, which is very often the case.[30–32]

Recently, we demonstrated the use of ten different LTC-QD pairs for ultrasensitive multiplexed diagnostics.[33] Herein, we show that the LTC-QD pairs can also be used as a multiplexed molecular ruler. A time-resolved analysis of five LTC-QD FRET pairs with different emission wave-

[*] Dipl.-Chem. F. Morgner, Dr. S. Stufler, Dr. N. Hildebrandt[+]
NanoPolyPhotonik
Fraunhofer Institut für Angewandte Polymerforschung
Geiselbergstrasse 69, 14476 Potsdam-Golm (Germany)
E-mail: niko.hildebrandt@iap.fraunhofer.de
Dipl.-Chem. D. Geißler, Prof. Dr. H.-G. Löhmannsröben
Physikalische Chemie, Universität Potsdam
Karl-Liebknecht-Strasse 24–25, 14476 Potsdam-Golm (Germany)
Dr. N. G. Butlin
Lumiphore Inc.
4677 Meade St., Suite 216, Richmond, CA 94804 (USA)
[+] Current address:
Institut d'Electronique Fondamentale
Bâtiment 220, Université Paris-Sud 11
F-91405 Orsay Cedex (France)
E-mail: niko.hildebrandt@u-psud.fr

[**] We would like to thank the European Commission for financial support (FP7 Collaborative Project NANOGNOSTICS-HEALTH-F5-2009-242264 and FP6 Specific Targeted Research Project POC4 Life-LSHB-CT-2007-037933) and Dr. Loïc J. Charbonnière for a fruitful discussion about the manuscript.

Supporting information for this article is available on the WWW under http://dx.doi.org/10.1002/anie.201002943.

Table 1: Biot-QD dimensions and average donor–acceptor distances *A* and *B*.[a]

Biot-QD		529	565	604	653	712
core/shell size	$x=y$	1.5–2	2.1[b]	2	3	3
	z	1.5–2	2.75[b]	4.7	6	6
overall size	$x=y$	6	6.8	7.2	8.1	8.35
	z	6	7.4	9.9	11.1	11.35
hydrodynamic radius		6	7	8	9	9.25
A		–	6.3	6.7	7.6	7.85
B		6.5	8	9	10	10.25

[a] Core/shell sizes (radial or ellipsoidal semiaxes) and hydrodynamic radii were provided by Invitrogen. Overall size ellipsoidal semiaxes (x, y, and z) were calculated from the hydrodynamic radii a, assuming an equal length of coated polymers over the entire QD surface and the same volume of sphere and ellipsoid ($a^3=xyz$). All values are given in nm. Dimensions are shown in the Supporting Information, Figure S5. [b] The radius of 2.3 nm provided by Invitrogen was corrected for slight elongation, as shown in Ref. [30].

lengths allowed us to measure the overall dimensions (shape and size) of five different biocompatible QDs. Importantly, all FRET pairs were excited with the same wavelength. Our LTC-QD spectroscopic ruler allows the multiplexed measurement of different QDs with coatings of various sizes. The experiments were performed under physiological conditions with standard spectroscopic equipment. The LTC-QD FRET ruler is well-suited for measurements ranging from bare semiconductor QDs up to QDs with thick coatings. Moreover, the different LTC-QD FRET systems can become applicable for long-distance multiplexed intracellular measurements if thin QD coatings are used. Due to the bright luminescence and the efficient FRET of our donor–acceptor pairs, all of the measurements can be performed at very low (sub-nanomolar) concentrations.

To validate our multiplexed spectroscopic ruler technique, we chose a commercially available LTC (Lumiphore Inc., USA) as FRET donor in combination with five different commercial QDs (Invitrogen, USA) as acceptors. Taking advantage of the large difference in luminescence lifetime for LTCs (ms) and QDs (ns), both donor (LTC) and acceptor (QD) time-resolved luminescence decay curves were used for distance calculations, thus giving an independent control of our results. The LTC Lumi4-Tb is based on an isophthalamide structure[34,35] and was labeled to streptavidin (sAv) with Lumi4-Tb/sAv = 4.4. Lumi4-Tb is very stable and reliable in different physiological buffers with very good spectroscopic performance. The luminescence decay time was (2.5 ± 0.1) ms and the luminescence quantum yield ($\Phi=\Phi_{sens}\Phi_{Tb}$) was 0.6 ± 0.1 with $\Phi_{sens}=0.83\pm0.17$ for sensitization from ligand to Tb^{3+} and $\Phi_{Tb}=0.72\pm0.15$ for the Tb^{3+} luminescence. Absorption and emission spectra can be found in the Supporting Information, Figure S1. The five different QDs were selected to fit their emission wavelengths within the gaps of the terbium emission spectra, resulting in low spectroscopic cross-talk between independent detection channels (Supporting Information, Figure S2). The emission maxima were 529, 565, 604, 653, and 712 nm. The CdSe/ZnS (CdSeTe/ZnS in the case of QD712) core/shell QDs range from spheres with circa 3 nm diameter (QD529) to rather elongated shapes (ellipsoids) with 6 and 12 nm axes (QD712). Each QD is polymer-coated and has 5 to 7 biotin molecules (Biot) attached to its surface, resulting in Biot-QDs with different shapes and sizes (Table 1).

Our experiments were performed in solutions of increasing concentrations of Biot-QDs with constant concentrations of Lumi4-Tb-sAv, thereby forming increasing amounts of stable bioconjugates of Lumi4-Tb-sAv-Biot-QD due to the strong affinity between Biot and sAv. Working with several different concentrations of the FRET complexes has two advantages. First, we have access to many independent luminescence decay curves for the same LTC-QD FRET system, which results in a better statistical characterization of the fitted decay times. Second, we can validate the concentration limits for receiving luminescence signals with a sufficient intensity for a quantitative analysis of the donor–acceptor distances. For the validation of our spectroscopic ruler approach, the LTC-QD distances were estimated by the structural information of the Biot-QDs and the LTC-sAv (Table 1; Supporting Information, Figure S5). The random labeling of Lumi4-Tb all over the sAv and the elongated shape of the QDs result in a donor–acceptor distance distribution. In theory, the FRET point-dipole approximation was found to be applicable for semiconductor quantum dots.[36] Thus, we defined a relatively small imaginary surface of 1 nm in diameter inside the QD cores as FRET acceptor plane. For the spherical QD529, we selected one FRET donor plane (1 nm out of the Biot-QD529 surface) representing the average donor–acceptor distance *B*. For the ellipsoidal QDs, we defined two energy donor planes, one being the closest possible distance (small ellipsoidal semiaxis) and the other being an average long distance (1.5 nm out of the hydrodynamic surface). Thus, there are two average donor–acceptor distances *A* (short) and *B* (long) between the QD–acceptor plane and the two LTC–donor planes.

To determine the donor–acceptor distances r by spectroscopic ruler experiments, we performed a time-resolved analysis of the Lumi4-Tb and the QD luminescence signals. Determination of r requires the luminescence decay times of the donor (Lumi4-Tb) in absence of the acceptor (QD), τ_D, and in the presence of the acceptor, τ_{DA}. Due to the large difference in excited-state lifetimes between the LTC donor and the QD acceptor, the FRET-sensitized acceptor decay time is $\tau_{AD}=\tau_{DA}$.[37] This offers the advantage of having access to distance information by analyzing the FRET-sensitized QD acceptor luminescence decay, which is a necessary requirement for a multiplexed measurement with one donor that is quenched by several acceptors. The donor–acceptor distances r can be calculated according to Equation (1):

$$\frac{R_0^6}{R_0^6+r^6}=1-\frac{\tau_{DA}}{\tau_D}=\eta_{FRET} \quad (1)$$

with the Förster radius R_0 and the FRET efficiency η_{FRET}. All of the FRET systems were measured successively with 10 different Lumi4-Tb-sAv/Biot-QD ratios. As luminescence decay times are concentration-independent, each of the recorded time traces can be used for the distance determi-

nation. Figure 1 shows some representative decay curves of Lumi4-Tb-sAv and Biot-QD653 luminescence after background subtraction.

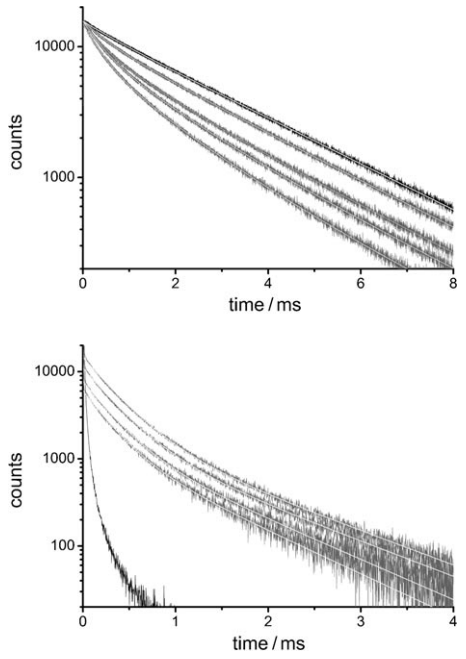

Figure 1. Representative lifetime traces for the system Lumi4-Tb-sAv-Biot-QD653 and mathematical fits (thin white lines). Top: Background-subtracted Lumi4-Tb emission at (542 ± 10) nm. The black monoexponential curve represents pure Lumi4-Tb-sAv (0.2 nM). Increasing Biot-QD concentrations (decreasing Lumi4-Tb-sAv per Biot-QD ratios *X*) lead to FRET quenching of the Lumi4-Tb luminescence. Biot-QD653 concentrations are, from top to bottom: 7 pM (*X* = 30), 30 pM (*X* = 6), 170 pM (*X* = 1.2), and 330 pM (*X* = 0.6). Bottom: Background- and Lumi4-Tb-signal-corrected QD653 emission at (660 ± 10) nm. Pure Lumi4-Tb-sAv does not show any signal. Increasing Biot-QD concentrations lead to FRET sensitization of the QD653 luminescence. Biot-QD653 concentrations are, from bottom to top: 7 pM (*X* = 30), 17 pM (*X* = 12), 30 pM (*X* = 6), and 70 pM (*X* = 3). The black curve shows the luminescence signal from 330 pM of pure Biot-QD (without Lumi4-Tb-sAv).

The addition of Biot-QD653 to Lumi4-Tb-sAv leads to Lumi4-Tb luminescence quenching, and new shorter time components become clearly visible within the decay curves. The QD653 luminescence curves also show a new decay time component. The intensity increases with Biot-QD653 addition owing to FRET sensitization. Although the luminescence decay of directly excited QDs is in the 10 to 100 ns timescale, the very strong QD luminescence (from direct QD excitation) leads to a decay curve that is still present after some milliseconds in the case of very high Biot-QD653 concentrations (Figure 1, bottom). However, the FRET-sensitized Biot-QD653 curves are in a much lower concentration range and luminescence from directly excited QDs can be neglected. Thus, the QD653 luminescence must result from FRET sensitization by Lumi4-Tb. The FRET experiments were performed for all Lumi4-Tb-sAv-Biot-QD combinations, and luminescence decay times (τ_D, τ_{DA}, and τ_{AD}), FRET efficiencies (η_{FRET}), and donor–acceptor distances (r) were calculated from the decay curves by multiexponential fitting procedures. (For details of the decay time analysis, see Ref. [23] and the Experimental Section; all measured and calculated values can be found in the Supporting Information, Table S1.) As the time-resolved analysis of the QD acceptor luminescence is necessary for a multiplexed investigation, we first fitted the different QD luminescence decay curves for τ_{DA1} and τ_{DA2}. The two average distances r_1 and r_2 were then calculated using Equation (1). To approve the values from the acceptor analysis, the Lumi4-Tb donor luminescence decay curves were fitted for τ_D and two average τ_{DA1} and τ_{DA2} with τ_D kept constant for all of the concentrations. This donor analysis confirmed the results from the acceptor decays.

Figure 2 shows the results from the time-resolved spectroscopic ruler (acceptor luminescence decay curves) compared to the Biot-QD structural information from Table 1.The results of the FRET ruler measurements fit very well the structural expectations ($A <$ hydrodynamic radius of Biot-QD $< B$). The increasing donor–acceptor distances resulting from the increasing Biot-QD sizes could be detected quite precisely by the time-resolved FRET measurements, even at low sub-nanomolar concentrations. Moreover, a distinction between the spherical and elongated QDs was possible.

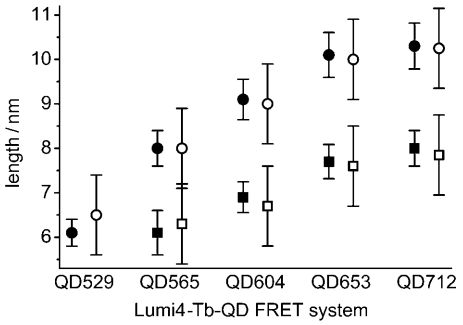

Figure 2. Distance measurements performed with the different Lumi4-Tb-QD FRET systems. The open symbols represent the average donor–acceptor reference distances *A* (squares) and *B* (circles) from the QD dimensions, with an estimated uncertainty of ± 1 nm. The filled symbols represent the distances calculated from time-resolved analysis (molecular ruler).

To evaluate the three-dimensional shape of the QDs (cigar-shaped with two short axes or pancake-shaped with two long axes), we took a closer look at the contributions of the different pre-exponentials and intensities of the multiexponentially decaying luminescence curves (Figure 1). This analysis allows the measurement of the concentration fractions (pre-exponentials) of Lumi4-Tb complexes at the two separation distances (A and B, or r_1 and r_2) from the QD center with their respective luminescence intensities (product of pre-exponentials and decay times). The increasing luminescence intensity ratio of the short- and long-distance component with QD size (Supporting Information, Figure S4) shows the growing proportion of the short-lived component to

the overall luminescence. Also the fraction of Lumi4-Tb complexes positioned at the short distance from the QD core increases with QD size (Figure 3). As the average surface to

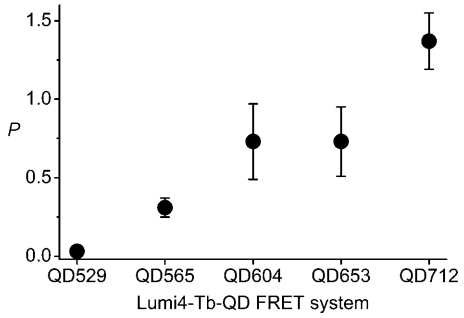

Figure 3. Concentration ratio *P* of Lumi4-Tb complexes at the short distance *A* and the average long distance *B* calculated from the pre-exponential factors of the double-exponential QD decay curves. The increasing relative amount of the short-distance component is caused by the QD elongation along the *z* axis with increasing size, as confirmed by TEM images.[30] The analysis of *P* allows a three-dimensional size evaluation of the QDs.

center distance of a cigar-shaped ellipsoid is $a=(x\,y\,z)^{1/3}$, the relative amount of Biot-sAv binding sites close to the short-axes distances $x=y$ increases with increasing z (elongation along the z axis). The increase of the relative amount of short- to long-distance components in the exponential luminescence decays is thus a very good evidence of a cigar-shaped elongation of the QDs with increasing size.[30] Moreover, the intensity and the concentration fractions of the short QD529 component are negligible compared to the long ones, which confirms the spherical shape of these QDs with only one average distance *B* (Table 1; all pre-exponential and intensity values and their calculation can be found in the Supporting Information, Table S1).

In conclusion, we have demonstrated a novel QD-based multiplexed technique for low-concentration spectroscopic ruler applications. Extremely large FRET distances (with Förster radii of up to 11 nm) can be measured for all LTC-QD FRET pairs without the aid of additional FRET enhancers.[38] The present work is, to our knowledge, the first demonstration of a multiplexed FRET molecular ruler. This novel approach offers the significant benefits of simultaneously analyzing different biofunctional events with high sensitivity and speed. Moreover, our method allows the multiplexed measurement of very accurate size and shape information of functionalized quantum dots under physiological conditions. Our current research focus is directed towards bringing our proof-of-principle into real-life applications, such as biostructural analysis, live-cell investigations or real-time PCR, and towards fundamental research concerning nano-FRET biosystems. Using lanthanide complexes and semiconductor quantum dots for biological FRET investigations offers many advantages. We believe that our demonstration of a highly sensitive multiplexed FRET spectroscopic ruler will become important for many applications in the fields of life sciences and nanotechnology.

Experimental Section

Lumi4-Tb was delivered from Lumiphore in the streptavidin labeled form with a labeling ratio of 4.4 Lumi4-Tb/sAv. Luminescence decay times were measured in 50 mM borate buffer (pH 8.3) containing 2% bovine serum albumin (BSA) and 0.5 M KF. The sizes of the CdSe/ZnS core/shell quantum dots were analyzed with TEM and the hydrodynamic diameters of the Biot-QDs were analyzed with exclusion chromatography on HPLC. Both methods were performed by Invitrogen. The sample volume was 150 μL for all of the spectroscopic measurements. All samples contained 0.2 nM Lumi4-Tb-sAv except for the control measurements with pure buffer and pure Biot-QDs (330 pM). Biot-QD concentrations were 7, 17, 30, 70, 100, 130, 170, 200, 270, and 330 pM. All samples were excited with a pulsed nitrogen laser system (SpectraPhysics, USA) with 100 shots at a 20 Hz repetition rate and a pulse energy of circa 50 μJ (at the sample) at 337.1 nm. A modified KRYPTOR immunoanalysis plate reader (Cezanne, France) with two photomultiplier-tube (PMT) detection channels and changeable bandpass filters (Delta, Denmark and Semrock, USA) was used for the spectroscopic ruler measurements (for the detection setup , see the Supporting Information, Figure S6). For all of the samples, the Lumi4-Tb and the QD emission were recorded simultaneously in the two PMT channels (Lumi4-Tb channel and QD channel). Time traces were recorded from 0 to 8 ms after the excitation pulse in 4000 channels of 2 μs. Mathematical fits were performed with FAST software (Edinburgh Instruments, UK).

Received: May 15, 2010
Published online: August 30, 2010

Keywords: biosensors · FRET · quantum dots · spectroscopic rulers · terbium

[1] K. E. Sapsford, L. Berti, I. L. Medintz, *Angew. Chem.* **2006**, *118*, 4676; *Angew. Chem. Int. Ed.* **2006**, *45*, 4562.
[2] P. R. Selvin, *Nat. Struct. Biol.* **2000**, *7*, 730.
[3] H. Bazin, M. Préaudat, E. Trinquet, G. Mathis, *Spectrochim. Acta Part A* **2001**, *57*, 2197.
[4] L. Stryer, *Annu. Rev. Biochem.* **1978**, *47*, 819.
[5] L. Stryer, R. P. Haugland, *Proc. Natl. Acad. Sci. USA* **1967**, *58*, 719.
[6] V. V. Didenko, *Biotechniques* **2001**, *31*, 1106.
[7] E. A. Jares-Erijman, T. M. Jovin, *Nat. Biotechnol.* **2003**, *21*, 1387.
[8] B. Schuler, *ChemPhysChem* **2005**, *6*, 1206.
[9] P. G. Wu, L. Brand, *Anal. Biochem.* **1994**, *218*, 1.
[10] D. M. Chudakov, S. Lukyanov, K. A. Lukyanov, *Trends Biotechnol.* **2005**, *23*, 605.
[11] B. N. G. Giepmans, S. R. Adams, M. H. Ellisman, R. Y. Tsien, *Science* **2006**, *312*, 217.
[12] E. A. Jares-Erijman, T. M. Jovin, *Curr. Opin. Chem. Biol.* **2006**, *10*, 409.
[13] I. L. Medintz, *Trends Biotechnol.* **2006**, *24*, 539.
[14] A. Miyawaki, *Dev. Cell* **2003**, *4*, 295.
[15] H. W. Ai, K. L. Hazelwood, M. W. Davidson, R. E. Campbell, *Nat. Methods* **2008**, *5*, 401.
[16] D. M. Grant, W. Zhang, E. J. McGhee, T. D. Bunney, C. B. Talbot, S. Kumar, I. Munro, C. Dunsby, M. A. A. Neil, M. Katan, P. M. W. French, *Biophys. J.* **2008**, *95*, L69.
[17] A. Piljic, C. Schultz, *ACS Chem. Biol.* **2008**, *3*, 156.
[18] Y. Niino, K. Hotta, K. Oka, *PLoS ONE* **2009**, *4*, e6036.
[19] L. J. Charbonnière, N. Hildebrandt, *Eur. J. Inorg. Chem.* **2008**, 3241.
[20] N. Hildebrandt, H.-G. Löhmannsröben, *Curr. Chem. Biol.* **2007**, *1*, 167.

[21] L. J. Charbonnière, N. Hildebrandt, R. F. Ziessel, H.-G. Löhmannsröben, *J. Am. Chem. Soc.* **2006**, *128*, 12800.
[22] N. Hildebrandt, L. J. Charbonnière, M. Beck, R. F. Ziessel, H.-G. Löhmannsröben, *Angew. Chem.* **2005**, *117*, 7784; *Angew. Chem. Int. Ed.* **2005**, *44*, 7612.
[23] N. Hildebrandt, L. J. Charbonnière, H.-G. Löhmannsröben, *J. Biomed. Biotechnol.* **2007**, Article ID 79169.
[24] B. W. Van der Meer, G. Coker, S. Y. S. Chen, *Resonance Energy Transfer: Theory and Data*, VCH, New York, **1994**.
[25] G. L. Liu, Y. D. Yin, S. Kunchakarra, B. Mukherjee, D. Gerion, S. D. Jett, D. G. Bear, J. W. Gray, A. P. Alivisatos, L. P. Lee, F. Q. F. Chen, *Nat. Nanotechnol.* **2006**, *1*, 47.
[26] C. Sönnichsen, B. M. Reinhard, J. Liphardt, A. P. Alivisatos, *Nat. Biotechnol.* **2005**, *23*, 741.
[27] T. D. Lacoste, X. Michalet, F. Pinaud, D. S. Chemla, A. P. Alivisatos, S. Weiss, *Proc. Natl. Acad. Sci. USA* **2000**, *97*, 9461.
[28] S. Weiss, *Science* **1999**, *283*, 1676.
[29] X. Michalet, T. D. Lacoste, S. Weiss, *Methods* **2001**, *25*, 87.
[30] B. N. G. Giepmans, T. J. Deerinck, B. L. Smarr, Y. Z. Jones, M. H. Ellisman, *Nat. Methods* **2005**, *2*, 743.
[31] L. Jauffred, L. B. Oddershede, *Nano Lett.* **2010**, *10*, 1927.
[32] E. Oh, M. Y. Hong, D. Lee, S. H. Nam, H. C. Yoon, H. S. Kim, *J. Am. Chem. Soc.* **2005**, *127*, 3270.
[33] D. Geißler, L. J. Charbonnière, R. F. Ziessel, N. G. Butlin, H. G. Löhmannsröben, N. Hildebrandt, *Angew. Chem.* **2010**, *122*, 1438; *Angew. Chem. Int. Ed.* **2010**, *49*, 1396.
[34] M. K. Johansson, R. M. Cook, J. D. Xu, K. N. Raymond, *J. Am. Chem. Soc.* **2004**, *126*, 16451.
[35] S. Petoud, S. M. Cohen, J. C. G. Bünzli, K. N. Raymond, *J. Am. Chem. Soc.* **2003**, *125*, 13324.
[36] C. Curutchet, A. Franceschetti, A. Zunger, G. D. Scholes, *J. Phys. Chem. C* **2008**, *112*, 13336.
[37] B. Valeur, *Molecular Fluorescence: Principles and Applications*, Wiley-VCH, Weinheim, **2002**.
[38] I. Gryczynski, J. Malicka, Z. Gryczynski, J. R. Lakowicz, C. D. Geddes, *J. Fluoresc.* **2002**, *12*, 131.

